J. Membrane Biol. 136, 113–124 (1993)

The Journal of
Membrane
Biology
© Springer-Verlag New York Inc. 1993

Effects of D_2O on Permeation and Gating in the Ca^{2+}-Activated Potassium Channel from *Chara*

I.I. Pottosin[1], P.R. Andjus,[2] D. Vučelić[3], G.N. Berestovsky[1]

[1]Institute of Cell Biophysics, Russian Academy of Sciences, Pushchino, Moscow region, 142292, Russia
[2]Institute of General and Physical Chemistry, P.O.B. 551, Studentski trg 12, 11000 Belgrade, Yugoslavia
[3]Department of Physical Chemistry, School of Physical Chemistry, P.O.B. 550, 11000 Belgrade, Yugoslavia

Received: 24 November 1992/Revised: 21 May 1993

Abstract. We studied the effects of H_2O/D_2O substitution on the permeation and gating of the large conductance Ca^{2+}-activated K^+ channels in *Chara gymnophylla* droplet membrane using the patch-clamp technique. The selectivity sequence of the channel was: $K^+ > Rb^+ \gg Li^+$, Na^+, Cs^+ and Cl^-. The conductance of this channel in symmetric 100 mM KCl was found to be 130 pS. The single channel conductance was decreased by 15% in D_2O as compared to H_2O. The blockade of channel conductance by cytosolic Ca^{2+} weakened in D_2O as a result of a decrease in zero voltage Ca^{2+} binding affinity by a factor of 1.4. Voltage-dependent channel gating was affected by D_2O primarily due to the change in Ca^{2+} binding to the channel during the activation step. The Hill coefficient for Ca^{2+} binding was 3 in D_2O and around 1 in H_2O. The values of the Ca^{2+} binding constant in the open channel conformation were 0.6 and 6 μM in H_2O and D_2O, respectively, while the binding in the closed conformation was much less affected by D_2O. The H_2O/D_2O substitution did not produce a significant change in the slope of channel voltage dependence but caused a shift as large as 60 mV with 1 mM internal Ca^{2+}.

Key words: D_2O—K^+ channel—Calcium and voltage gating—Patch clamp—Cytoplasmic drop—*Chara*

Introduction

The H_2O/D_2O substitution has been previously used on excitable membranes to examine the ion channel gating mechanisms (Conti & Palmieri, 1968; Schauf & Bullock, 1979; Schauf, 1983) or to define the rate-limiting steps in channel permeation (Andersen, 1983; Lewis, 1984; Brink, 1984). In these studies, the magnitude of the changes in channel kinetic parameters induced by these isotope substitutions did not exceed a factor of 2. However, D_2O effects of larger magnitude were also observed, indicating a qualitatively different behavior in the examined system. Thus, for instance, externally applied D_2O abruptly decreased transepithelial potential in the frog skin, similar to the effect of a hyperosmotic stress (Lindley, Hoshiko & Leb, 1964). Recently, D_2O was shown to induce an action potential in the giant cell of the freshwater alga *Chara,* accompanied by a large K^+ efflux (Andjus & Vučelić, 1990). This was ascribed to a D_2O-induced activation of Ca^{2+} and Cl^- channels in the cell membrane (Andjus et al., 1990), while the effects of D_2O on K^+ channels were not studied in detail.

The large conductance K^+ channel of *Chara* droplet membrane is one of the first ionic channels in plants studied by the patch-clamp technique (Lühring, 1986) and also, one of the best characterized. At a low concentration of the permeant ion, its permeation was shown to be limited by diffusion in the region external to the pore (Laver, Fairley & Walker, 1989; Pottosin, 1990). The channel was activated by voltage and micromolar cytosolic Ca^{2+} (Laver & Walker, 1987, 1991), while larger concentrations of Ca^{2+} blocked the channel (Laver, 1990). Thus, a study was begun to investigate the gating mechanisms, which could underlay the previously observed large D_2O effects on this channel (Andjus et al., 1990), compared to the voltage-dependent channels of a different origin.

Correspondence to: P.R. Andjus

Materials and Methods

Plant material: Internodal cells of *C. gymnophylla* were kept in APW prior to experiment. Cells of 1–2 cm were selected, gently dried on filter paper and used in further preparation procedures. A number of comparative experiments were performed on a related *Characean* species, *Nitellopsis obtusa*.

Preparation: Cytoplasmic droplets were obtained by the modified method of Bertl (1989). Namely, the cells were cut at both ends and internally perfused by immersion in a solution containing (mM) 100 NaCl or KCl, 0.01 or 1 $CaCl_2$, and 10 HEPES-KOH (pH 7.2). Droplets were spontaneously formed in the released cell sap and those of 50–200 μm in diameter were used in patch-clamp experiments. Similar preparations were also obtained according to the alternative method of Lühring (1986).

Solutions: In most of the experiments, pipette and bath solutions were initially the same, containing (mM) 100 KCl, 0.5 EDTA, 1.5 $CaCl_2$, 5–10 HEPES-KOH (pH 7.2, pD = pH + 0.4 = 7.2). Prior to use, pipette solutions were filtered with a 0.22 μm Millipore filter.

In other experiments, free Ca^{2+} concentrations at the cytoplasmic side were adjusted using Ca^{2+} buffer solutions. Ca^{2+} buffer solutions were prepared with (mM) 100 KCl, 10 HEPES-KOH (pH 7.2), 1 EGTA, 5 citric acid, 1 $MgCl_2$. Thus, the adjusted Ca^{2+} concentrations, total and free (in parentheses) were calculated to be (in μM): 10 (0.0016), 405 (0.1) 676 (0.3), 893 (1.0), 1,025 (3.2), 1,200 (10), 1,925 (50). Stability constants for the binding of H^+, Mg^{2+} and Ca^{2+} to EGTA and citrate were taken from Durham (1983). The lowest Ca^{2+}-free concentration was calculated by taking into account 10 μM Ca^{2+} contamination in the solution without EGTA, citric acid and Mg^{2+}, as directly measured with a Ca^{2+}-selective electrode. It was necessary to test the shifts of pK values of EGTA and citric acid in D_2O (Lobyshev & Kalinichenko, 1978). As shown in Fig. 1, pK values for these acids shifted by 0.3–0.6 units to a more alkaline region, compared to the values in H_2O. The pK values in D_2O were used further for the correction of Ca^{2+} concentration in the buffer with D_2O.

Patch-clamp experiments: Micropipettes were made from hard borosilicate glass (Pyrex) with filament. The two-stage pulling procedure was used, with subsequent fire-polishing of pipette tips using a platinum ribbon. In further experiments, we used patch microelectrodes with tip openings of 1–2 μm in diameter and with resistances of 7–25 MΩ in standard 100 mM KCl solution.

Electrical measurements were performed using an SKB Biopribor patch-clamp preamplifier (Pushchino, Russia), equipped with a 10 GΩ feedback resistance headstage with a current noise of 0.2 pA at 0–1 kHz. The largest measurable current was 200 pA and the holding potential range was ±200 mV. The reference and patch electrodes were filled with the same solution, and the electrode potential was corrected to zero before measurement. Command potentials were provided by the generator G-6 (Russia), in a form of rectangular (5–150 sec) or ramp wave (200 msec) pulses, with the amplitudes in the range of ±200 mV. A standard patch-clamp technique (Hamill et al., 1981) was used to obtain the excised outside-out and inside-out patches. Gigaseals in the range of 5–50 GΩ were formed by applying light suction of 5–10 cm H_2O. We obtained outside-out patches by rupturing the patch membrane in the cell-attached configuration with a 200 mV voltage pulse of 1–5 sec duration with subsequent withdrawal of the pipette, or by withdrawing the pipette after achieving the gigaseal and disrupting the inner membrane of the vesicle, formed on the tip, by a large voltage stimulus. Inside-out patches were obtained by briefly exposing the membrane vesicle to air. The sidedness of the patch membrane was checked by testing the effects of Ca^{2+} in the bath. The membrane potential difference is taken with respect to the outside of the membrane (cytoplasm minus exterior). The positive current is defined as positive charge flowing from the inside of the membrane (cytoplasmic side), unless otherwise stated. The current signals were filtered by a 6-pole Bessel filter setting at 1 kHz, displayed on an oscilloscope and continuously recorded on magnetic tape using an FM data recorder (TEAC MRC-10C, Japan). Calibrations were made at the beginning of each tape recording by applying a square-wave voltage signal of known amplitude. For the analysis of channel activity, the records were played back, digitized and averaged over 0.5–2.5 min intervals, using a Nicolett 527 Signal Averager (Tektronix, Beaverton, OR) and copied by an XY plotter for further evaluation of mean current amplitudes. Current-voltage (*I-V*) relationships of the channel in the open state were measured using ramp-wave voltage protocols and by subtracting the records with the channels closed from those with one open channel pres-

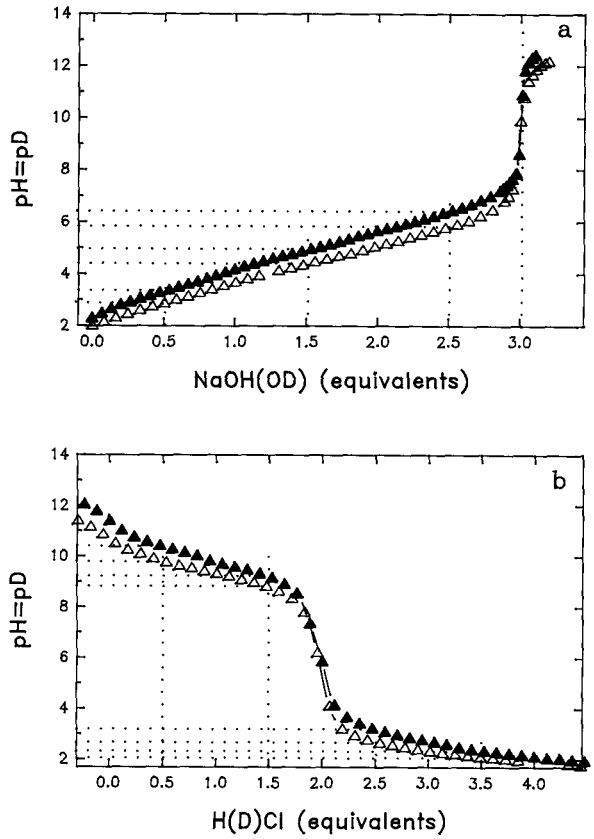

Fig. 1. Titration curves of the components of Ca^{2+} buffer solutions. (*a*) 0.1 M citric acid; (*b*) 0.01 M EGTA, open triangles: H_2O; filled triangles: D_2O. Citric acid was dissolved in H_2O or D_2O and titrated with 2 N NaOH(OD). EGTA was dissolved at slightly alkaline pH (pD), then titrated with NaOH(OD) to approach the alkaline buffer zone and titrated back with 1 N H(D) Cl. DCl and NaOD were prepared by dissolving or diluting NaOH and 10 N HCl, respectively, in 99.8% D_2O. The values of half-equivalence (pK) points in H_2O (D_2O) for citric acid are: 2.8(3.3); 4.4(4.9); 5.8(6.4) and for EGTA: 2.0(2.3); 2.7(3.2); 8.9(9.3); 9.8(10.4).

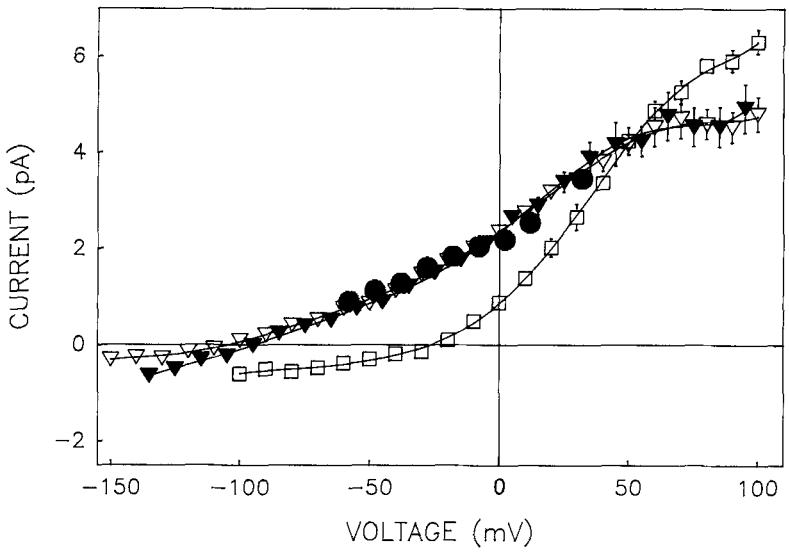

Fig. 2. Current-voltage relationships for the K^+ channel in outside-out patches in the presence of different alkali cations at the external side. KCl (100 mM) with 1 mM $CaCl_2$ was present at the internal side. Solution in the bath contained 100 mM of the following cations added as chlorides: Li^+ (filled triangles); Na^+ (open triangles); Rb^+ (squares); Cs^+ (circles). Unbroken curves are low-order polynomials, fitted to the data using least squares, and giving reversal potentials for Li^+, Na^+ and Rb^+ of (in mV) -95 ± 4, -109 ± 4, -25 ± 2, respectively.

ent, or by estimating the unitary current amplitude values from current fluctuations at the fixed potentials.

Results

Selectivity

Figure 2 shows the *I-V* relationships of the channel in outside-out patches with 100 mM KCl in the pipette and 100 mM of other alkali cations added as chlorides in the bath. According to the reversal potential (V_r) in these bi-ionic conditions, the obtained selectivity sequence (with relative permeabilities to K^+ in brackets) was: $K^+ > Rb^+$ (0.38 ± 0.08, $n = 3$) $\gg Li^+$ (0.025 ± 0.004, $n = 3$), Na^+ (0.014 ± 0.002, $n = 5$), Cs^+ (<0.005). According to the Goldman-Hodgkin-Katz equation, the relative permeabilities in parentheses (presented as mean ± SE over n patches) are the sum of cation and Cl^- permeabilities. Thus, since the lowest cation permeability was $P_{Na} = 0.014$ (*see above*), it could be estimated that $P_{Cl^-}/P_{K^+} < 0.014$. With 100/20 mM KCl gradient across the membrane, V_r was found to be -41 ± 1 mV ($n = 5$) in H_2O as expected for ideal K^+/Cl^- selectivity.

Effects of D_2O on Channel Conductance and its Attenuation by Cytosolic Ca^{2+}

The conductance of K^+ channels in the *Chara* droplet membrane was shown to be decreased by millimolar concentrations of cytosolic Ca^{2+} (Laver, 1990). Therefore, D_2O effects on channel *I-V* relationships at high (1 mM) and low (10 μM) Ca^{2+} concentrations in the pipette were analyzed on outside-out patches (Fig. 3). As shown in Fig. 3, D_2O applied to the external side of the membrane at low Ca^{2+} decreased both inward and outward currents by 15%, while at 1 mM Ca^{2+} it induced a similar change only in currents at negative potentials. The *I-V* relationships were usually measured within 1–3 min after solution substitution. No changes in the shape of *I-V* relationships were found after 10, 20, or 30 min of superfusion with a fresh D_2O solution at each indicated time (*not shown*). The *I-V* relationship at high Ca^{2+} was taken relative to that at low Ca^{2+} and fitted with the following equation (Woodhull, 1973):

$$I_{K+Ca}/I_K = \left\{1 + \frac{[Ca^{2+}]\exp(2\delta FV/RT)}{k_d(0)}\right\}^{-1} \quad (1)$$

where δ is a fraction of potential drop across the membrane towards the Ca^{2+} binding site, $k_d(0)$ is the binding constant for Ca^{2+} at zero potential, V is the membrane voltage, and F, R, T have their usual meanings. The values of $k_d(0)$ and δ were found to be 8 ± 1 mM and 0.25 ± 0.02, and 11 ± 2 mM and 0.26 ± 0.03 in H_2O and D_2O, respectively. Thus, H_2O/D_2O substitution mainly affected the Ca^{2+} binding affinity at zero voltage, decreasing it by a factor of 1.39 ± 0.25.

In a number of outside-out patches, the magnitude of the above effect was also estimated by averaging the slopes of *I-V* relationships at zero voltage. In H_2O the values of channel slope conductances, g_o, were found to be 130 ± 2 ($n = 9$) and 116 ± 2 pS ($n = 5$), at 10 μM and 1 mM Ca^{2+}, respectively. With the same patches in D_2O, g_o values were 111 ± 1 and 103 ± 2 pS, respectively. By dividing the difference between g_o at low and high Ca^{2+} with

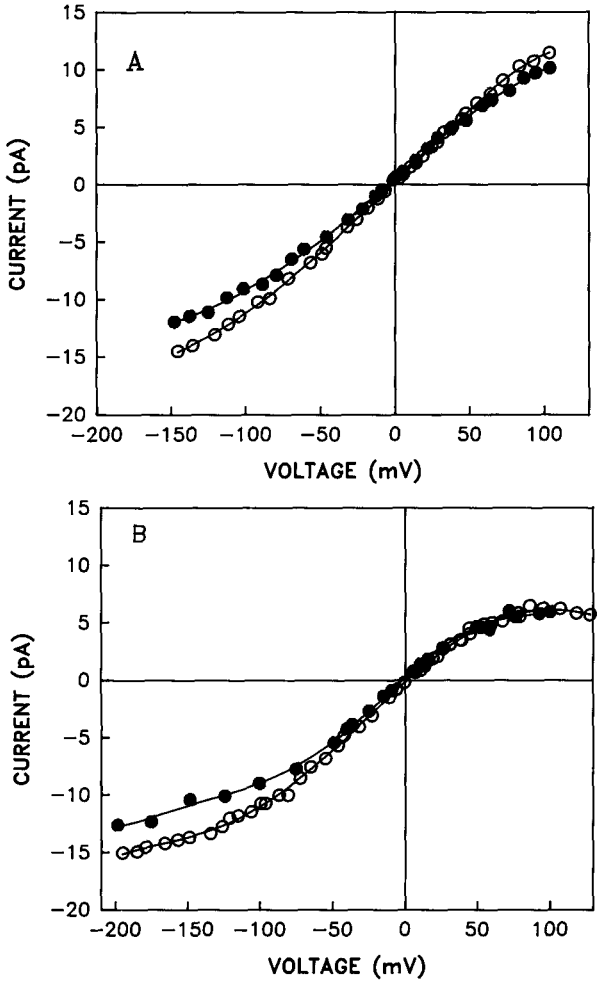

Fig. 3. Current-voltage relationships of *C. gymnophylla* K^+ channel in excised outside-out patches in symmetric 100 mM KCl. Ca^{2+} concentration in the pipette was 0.01 mM in (*A*) and 1 mM in (*B*). Symbols: open: H_2O, filled: D_2O. The unbroken curves are low-order polynomials fitted to the data using least squares.

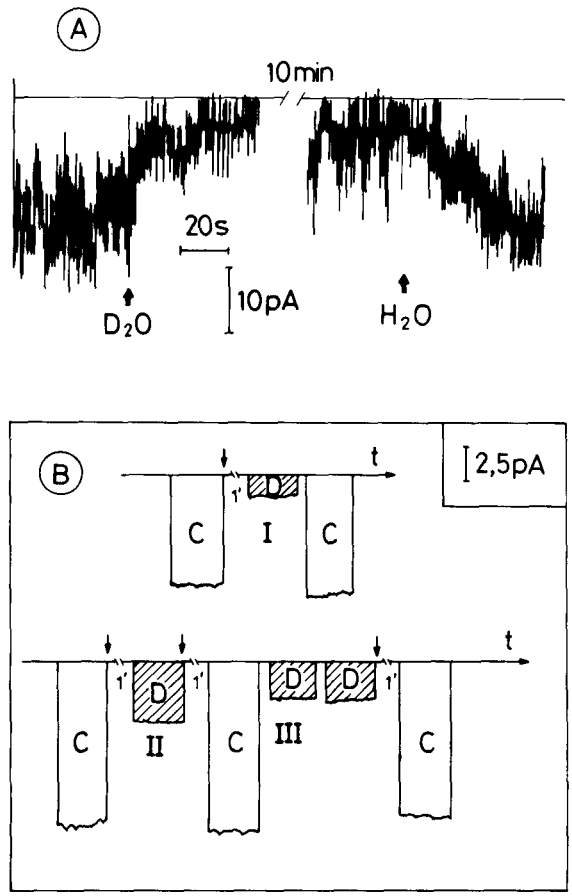

Fig. 4. Effect of external H_2O/D_2O substitution on the channel activity in the outside-out patches. $V_m = -50$ mV, K^+ and Ca^{2+} concentrations at both sides were 100 and 1 mM, respectively. (*A*) An example of the single channel recording with one cycle of $H_2O/D_2O/H_2O$ substitution. (*B*) Changes in the amplitude of the mean current passing through the patch with three K^+ channels, during three cycles of H_2O/D_2O substitutions (at arrows); C: Control (H_2O), D: D_2O; each bar represents an average over a 128 sec recording interval.

g_o at low Ca^{2+} the equilibrium constant, $k_d(0)$, for Ca^{2+} binding was obtained. This value in H_2O and D_2O, was 9 ± 2 and 13 ± 4 mM, respectively. These values differed by a factor 1.46 ± 0.48, in agreement with the previous ratio. When H_2O was replaced by D_2O at both sides (at 1 mM Ca^{2+}) the slope conductance value for the channel was 99 ± 3 pS (n = 3) which was close to that found with H_2O substituted by D_2O at the external side (*see above*).

Effects of H_2O/D_2O Substitution on K^+ Channel Activity at Fixed Ca^{2+} and Voltage

The effects of H_2O/D_2O substitution on the channel activity were measured at −50 mV with 1 mM Ca^{2+} at both sides. In outside-out patches, replacing H_2O with D_2O in the external solution caused an immediate decrease in channel activity which could be reversed by returning H_2O into the chamber (Fig. 4*A*). D_2O was not usually kept in the experimental chamber longer than 15 min. At the end of this period we did not find significant changes in the channel activity and the concentration of H_2O in the solution, exchanged for D_2O with the atmosphere, was less than 5%, as estimated with ^{1}H-NMR measurements. The values of mean current through a number of channels in the patch were obtained from the first cycle of $H_2O/D_2O/H_2O$ exchange, averaged over several minutes in H_2O and D_2O. In some patches, however, several successive cycles of $H_2O/D_2O/$

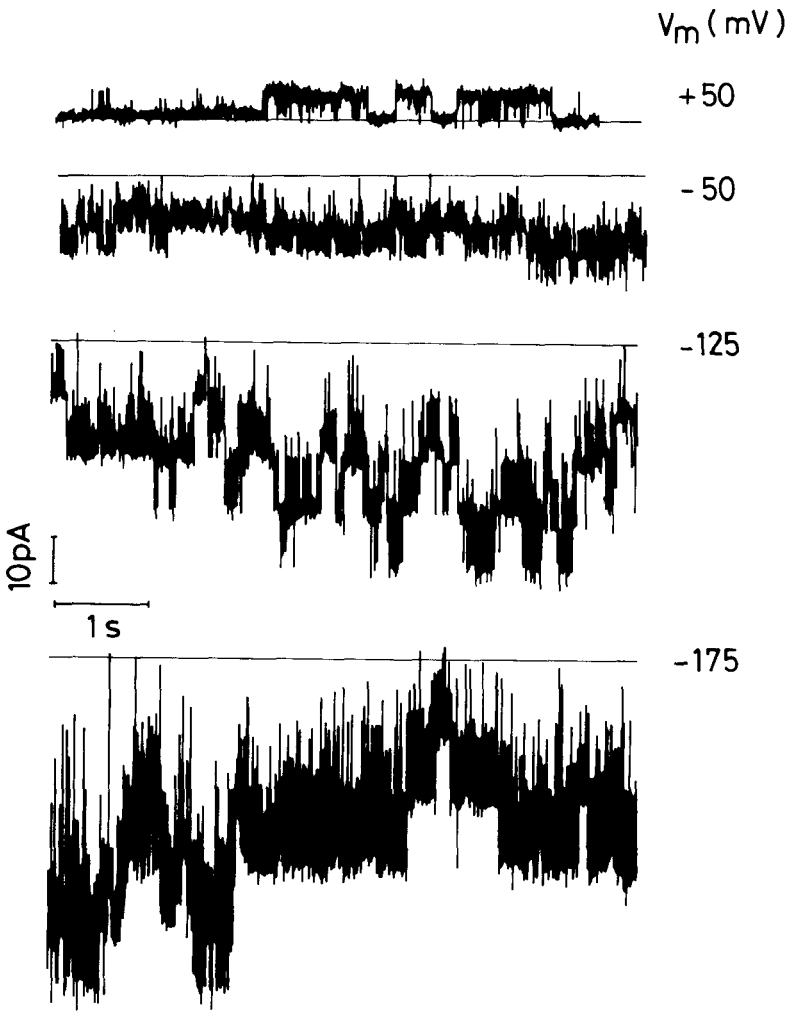

Fig. 5. Recording of single K^+ channel fluctuations in an outside-out patch, measured at various voltages. Ca^{2+} concentrations in the bath and in the pipette were 50 μM and 1 mM, respectively. Signals are filtered at 1 kHz. The current baseline is shown at each record (horizontal line). Everything else is the same as in legend to Fig. 4.

H_2O exchange could be performed and the example with three such cycles is shown in Fig. 4*B*.

The channel activity, designated as NP_o (N = number of channels; P_o = open channel probability) was expressed as I/i, where I is the mean current averaged over 0.5–2.5 min, and i the unitary current. The NP_o values obtained in D_2O were taken relative to H_2O before and after substitution to D_2O and averaged over a number of patches. This value of NP_o obtained from 11 outside-out patches for the *C. gymnophylla* K^+ channel was 0.42 ± 0.04, as compared to 0.39 ± 0.04 (n = 6) obtained for the K^+ channel in the related species *N. obtusa*.

Effects of Voltage and Cytosolic Ca^{2+} on the Channel Activity

Clamping the membrane to positive potentials produced longer channel closures, thus decreasing the mean number of the opened channels (Fig. 5). At large negative potentials (< − 150 mV) frequent brief channel closures appeared. Although this process could also decrease channel open probability, its contribution was not significant up to the highest attainable holding potential (−200 mV).

The decrease of cytosolic Ca^{2+} concentration apparently had the same effect as the stepping of membrane potential to positive values (Fig. 6*A*). Due to a large number of channels in most of the examined patches, it was not possible to perform an accurate analysis of Ca^{2+} and voltage effects on the distribution of channel open and close times. For the quantification of the observed channel activity, we used the mean number of opened channels (NP_o).

The effect of Ca_i^{2+} on channel activity was studied at −50 mV on inside-out patches, each containing 5–15 channels. In the course of the experiment, the bath medium was changed to a series of Ca^{2-}-buffered solutions with different pCa values. To check the reversibility of the effects of changed

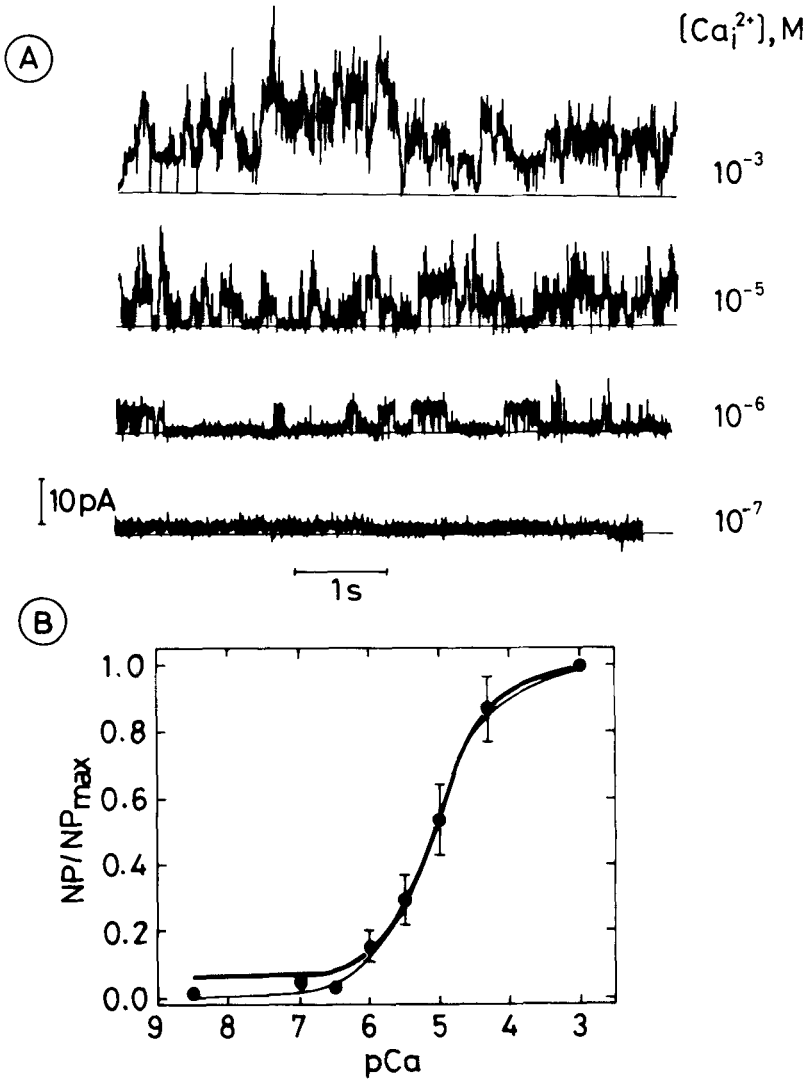

Fig. 6. Ca^{2+} activation of the large conductance K^+ channels in inside-out patches. $V_m = -50$ mV, symmetric 100 mM KCl and 1 mM $CaCl_2$ solutions. Note that the current convention is inverted (inward current is positive). (*A*) An example of the single channel current fluctuations in a patch at various concentrations of cytosolic Ca^{2+}. Current baseline is shown at the bottom of each record. Positive current is for positive charge moving from the cytoplasm. (*B*) Ca^{2+} dependence of the channel open probability at -50 mV, derived from three patches. The relative open probabilities were derived by taking the value of mean current through a number of K^+ channels at each patch averaged over several minutes at each Ca^{2+} concentration. Thick line is drawn to the data according to the Hill equation (Eq. (2) in the text). Thin line represents the fit to the following equation derived from the kinetic model (*see* Discussion):

$$P_o/P_{max} = (1 + \beta^\alpha)(1 + \gamma)/(1 + \beta^\alpha + \gamma(1 + \kappa\beta^\alpha)) \quad (4)$$

where $\gamma = \exp(z\delta F(V_x - V''_{1/2})/RT)$, $V_x = -50$ mV; $\beta = k_{d(open)}/[Ca^{2+}]$. The best fit gives the values of $k_{d(open)}$ and α equal to 0.6 μM and 1.1, respectively.

Ca^{2+} concentrations, we applied low Ca^{2+} after high Ca^{2+} and *vice versa*. Thus, each Ca^{2+} concentration was usually repeated 2–3 times at each patch. The channel activity relative to that at 1 mM Ca^{2+} plotted against pCa is shown in Fig. 6*B*. Fitting the data to the Hill equation of the form:

$$NP_o/NP_{o(max)} = \frac{([Ca^{2+}]/k_d)^\alpha}{1 + ([Ca^{2+}]/k_d)^\alpha} \quad (2)$$

gave the apparent values of the binding constant (k_d) and the Hill coefficient (α) for Ca^{2+} of 7.8 ± 0.6 μM and 0.92 ± 0.05, respectively.

Effects of D_2O on Voltage Dependence of the Channel Activity and its Modulation by Cytosolic Ca^{2+}

The effect of H_2O/D_2O substitution at the external side on the channel activity, as a function of voltage and cytosolic Ca^{2+} concentration, was measured on a number of outside-out patches each containing from 5–15 individual channels. The averaging of mean current and calculations of NP_o were done as above. In the pCa range of 3.0–6.0 the open probability dependence in H_2O showed saturation between -100 and -150 mV (Fig. 7). Thus, all NP_o values (in H_2O or D_2O) were given relative to the values averaged over the range of saturation potentials. However, at lower Ca^{2+} concentrations (pCa 7.0 and 8.8), there was no saturation in the examined potential range (Fig. 8), and the NP_o values were averaged for a number of patches and plotted against voltage. The unbroken curves in Figs. 7 and 8 are predictions of the effective number of opened channels using the Boltzmann distribution:

$$NP_o(V) = NP_{o(max)} \frac{\exp[z\delta F(V_{1/2} - V)/RT]}{1 + \exp[z\delta F(V_{1/2} - V)/RT]} \quad (3)$$

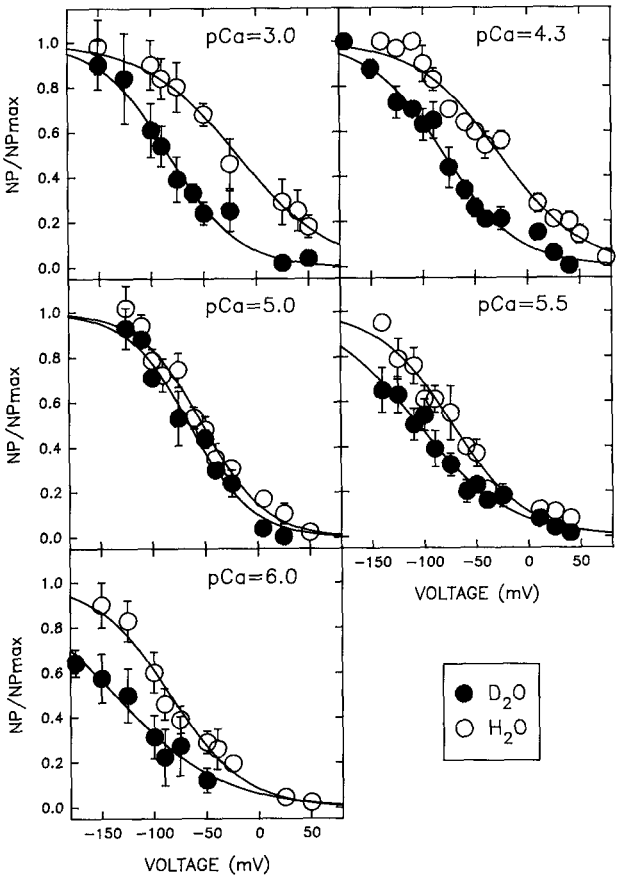

Fig. 7. The voltage dependence of the relative channel activity at different cytoplasmic Ca^{2+} concentrations. Data obtained from a total of 21 outside-out patches (with symmetric 100 mM KCl). Open circles: control (in H_2O); filled circles: H_2O in the bath is replaced by D_2O. Ca^{2+} concentrations shown are actual values in H_2O. Unbroken curves are the best fits of data using the Boltzmann distribution (*see text*). The values of parameters are given in Table 1.

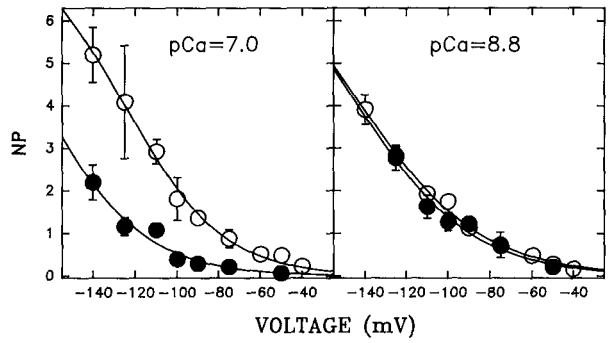

Fig. 8. The mean number of open channels at low Ca_i^{2+} as a function of voltage in H_2O and D_2O. Data of each panel are obtained from four outside-out patches. Unbroken curves are drawn according to the Boltzmann distribution (*see text*). The maximal mean number of open channels was estimated to be 8.0 ± 1.3 (n = 4) at pCa = 7.0 and 8.3 ± 2.5 (n = 4) at pCa = 8.8. Everything else is the same as in legend to Fig. 7.

where $NP_o(V)$ is channel activity at membrane voltage V, $NP_{o(\max)}$ is the maximal value of NP_o, $z\delta$ is the effective valence of the gating charge, $V_{1/2}$ is the value of the voltage at which half-maximal activation of the channel occurred, and other parameters have their usual meanings. The values of the parameters of channel voltage dependencies obtained at different Ca^{2+} concentrations are listed in Table 1. The results in Table 1 indicate that the slope of voltage dependence did not significantly change with the change of Ca^{2+} concentration or with the exchange of H_2O to D_2O. The values of $z\delta$ averaged over all Ca^{2+} concentrations were 0.79 ± 0.07 and 0.78 ± 0.07 in H_2O and D_2O, respectively. However, $V_{1/2}$ became more negative with the decrease of cytosolic Ca^{2+} concentration and in D_2O the channel activation was also shifted to negative potentials as compared to H_2O at the same Ca^{2+} concentration. The latter effect, however, was a complex function of Ca^{2+} concentration, being most significant at pCa = 3 and the least significant at pCa = 5.0 or 8.8 (Fig. 9, Table 2).

Discussion

Channel Identification

The K^+ channel studied here had a conductance of 130 pS in symmetric 100 mM KCl which could be compared with the conductance of the *C. australis* K^+ channel in similar ionic conditions (*see* Fig. 2 in Laver et al., 1989). The *C. gymnophylla* K^+ channel was blocked by internal Ca^{2+} with a k_d of 8 mM, and the Ca^{2+} binding site was found to be at the depth (δ) of 0.25 of the voltage drop across the membrane. These values, again, were close to those found for the *C. australis* K^+ channel (k_d = 15 mM; δ = 0.27; Laver, 1990). The permeabilities for Rb^+ and Na^+ relative to K^+ for the channel in *C. gymnophylla* were 0.38 and 0.014, respectively, comparable to the values of 0.33 and 0.01–0.02, respectively, for the *C. australis* K^+ channel (Lühring, 1986; Laver & Walker, 1991). Cytosolic Ca^{2+} concentration required to produce half-activation of the K^+ channel in *C. gymnophylla* was found to be 8 μM, while in *C. australis* it varied from 0.5 to 5 μM (Laver & Walker, 1991). Therefore, it could be concluded that the *C. gymnophylla* large conductance Ca^{2+}-activated K^+ channel is very similar or even identical to the K^+ channel, previously described in the *C. australis* droplet membrane.

Table 1. Parameters[a] of K^+ channel voltage gating in H_2O and D_2O as a function of cytoplasmic Ca^{2+}concentration[b]

pCa		3.0	4.3	5.0	5.5	6.0	7.0	8.8
H_2O	$z\delta$	0.58 ± 0.04	0.65 ± 0.05	0.87 ± 0.09	0.73 ± 0.06	0.73 ± 0.07	1.10 ± 0.17	0.87 ± 0.11
	$V_{1/2}$ (mV)	−18.0 ± 2.2	−27.1 ± 3.4	−52.1 ± 2.8	−73.6 ± 2.6	−84.5 ± 3.0	−124.9 ± 8.0	−143.7 ± 16.4
	n	3	3	5	4	4	4	4
D_2O	$z\delta$	0.78 ± 0.08	0.73 ± 0.06	0.88 ± 0.09	0.59 ± 0.04	0.51 ± 0.06	1.06 ± 0.16	0.91 ± 0.11
	$V_{1/2}$ (mV)	−83.1 ± 2.8	−80.3 ± 2.5	−64.3 ± 3.1	−106.3 ± 2.7	−137.2 ± 4.9	−164.0 ± 5.6	−145.3 ± 5.1
	n	3	3	3	3	3	3	3

[a] Mean ± SD for n patches. [b] (*See text for symbols*).

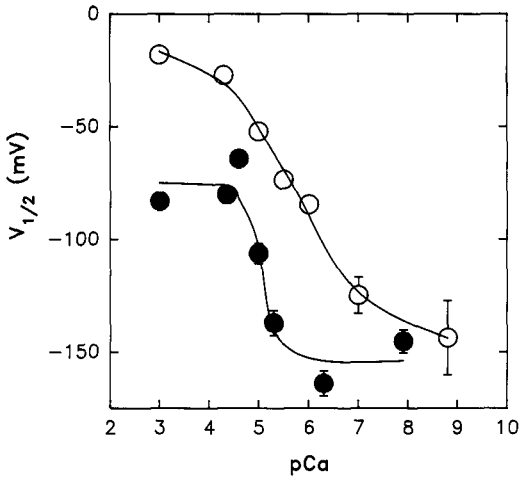

Fig. 9. The K^+ channel half-activation voltage as a function of cytoplasmic Ca^{2+} concentration. Open circles: outside-out patches in H_2O; filled circles: in D_2O. Data are taken from Figs. 7 and 8. Error bars are standard deviations obtained by fitting the data to the Boltzmann distribution (*see text*). pCa values in Ca^{2+} buffers with D_2O are corrected, assuming the shifts of pK by 0.3–0.6 units for citric acid and EGTA. Unbroken lines are drawn according to the equation derived from the kinetic scheme (*see* Discussion):

$$V_{1/2} = V''_{1/2} - \frac{RT}{z\delta F} \ln\left[\frac{1 + (k_{d(\text{open})}/[Ca^{2+}])^{\alpha}_{\kappa}}{1 + (k_{d(\text{open})}/[Ca^{2+}])^{\alpha}}\right] \quad (5)$$

The values of parameters are given in Table 2.

Effects of D_2O on the Channel Conductance and its Blockage by Internal Ca^{2+}

Deuterium oxide could, in principle, affect ionic channel conductance in two ways. First, by decreasing the conductivity of the solution in the vicinity of the channel pore, and secondly, for a channel with a somewhat restricted pathway for diffusion, by H/D exchange within a channel pore (Andersen, 1983; Brink, 1983). With the *Chara* K^+ channel it was found here that D_2O decreased the single channel conductance by 15%. This value is expected for a diffusion-limited channel conductance (Laver et al., 1989; Pottosin, 1990).

Table 2. Model parameters for the modulation of channel voltage dependence by Ca^{2+}[a]

Experimental condition	H_2O	D_2O
V' (mV)	−145 ± 5	−153 ± 10
V'' (mV)	−14 ± 6	−76 ± 9
α	0.7 ± 0.1	3.1 ± 1.9
$k_{d(o)}$ (μM)	0.6 ± 0.4	6 ± 2
$k_{d(c)}$ (μM)	30 ± 17	14 ± 5

[a] Fitted to the data of Fig. 9. V' and V'' are midpoint potentials for channel activation at 0 and infinite Ca^{2+}, α is the Hill coefficient, $k_{d(o)}$ and $k_{d(c)}$ are Ca^{2+} binding constants for the open and closed states, respectively.

In most of the experiments described here, the effect of external H_2O/D_2O substitution was studied. The following experimental facts, however, indicated that the internal side of the patch would soon also face a high concentration of D_2O: (i) in the absence of blocker (Ca_i^{2+}), externally applied D_2O reduced the inward and outward currents through the channel by the same extent, and this effect was stable in time; and (ii) the channel conductance in symmetric 100% D_2O solution was close to that measured with D_2O added only to the external side. The diffusion calculations (*see* Appendix) showed that D_2O concentration at the inner membrane side sharply increased (in a few seconds) after solution exchange and further on changed slowly (*see* Fig. 11). The measurements of *I-V* relationships of the channel were done in 1–3 min after solution exchange when D_2O concentration at the internal side is calculated to be between 86 and 99%, assuming that the permeability coefficient for water was in the range between $2.5 \cdot 10^{-3}$ and $1.5 \cdot 10^{-2}$ cm/sec, respectively (*see* Appendix). Thus, it appears that the relatively small effect of D_2O on the conductance of the *Chara* K^+ channel is not a consequence of a nonuniform distribution of D_2O at the opposite sides of the patch.

In the presence of higher concentrations of cytosolic Ca^{2+} the channel conductance decreased in a voltage-dependent manner, and the extent of this

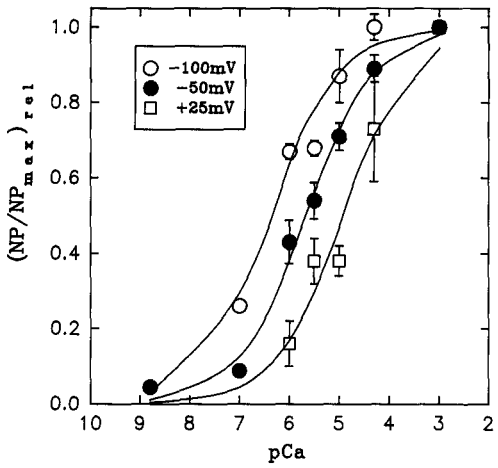

Fig. 10. The relative mean number of open K^+ channels as a function of cytosolic pCa at three different membrane potentials (+25, −50, −100 mV). Data were taken from Figs. 7 and 8 and normalized to the value at pCa 3.0. Curves were fitted to the Hill equation and gave k_d values of 12.1, 2.1 and 0.5 μM, respectively.

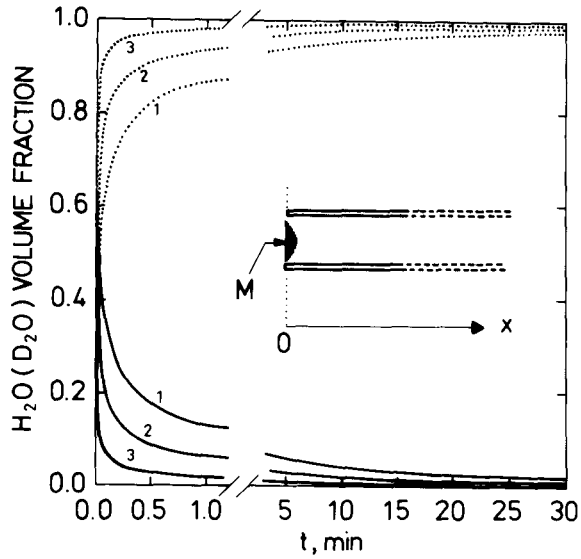

Fig. 11. Volume fraction of H_2O and D_2O at the internal surface of the patch as a function of time after H_2O/D_2O replacement in the external chamber. Calculations were made assuming the case of semi-infinite cylinder ($x \geq 0$) in which diffusion is in the axial direction with a membrane (M) at its tip (at $x = 0$), as shown in the inset. Curves for H_2O (unbroken lines) are calculated from Eq. (11A) and those for D_2O (dashed lines) are calculated assuming a constant sum of volume fractions of H_2O and D_2O. Coefficient of selfdiffusion of water is $D = 2 \cdot 10^{-5}$ cm^2 sec^{-1}, and the permeability coefficient is (in cm sec^{-1}): $P = 2.5 \cdot 10^{-3}$ (curve 1); $P = 5 \cdot 10^{-3}$ (curve 2); and $P = 1.5 \cdot 10^{-2}$ (curve 3; *see text for further explanation*).

blockade was found here to be different in H_2O as compared to D_2O. H_2O/D_2O substitution did not change the electrical distance for Ca^{2+} movement towards its binding site within the channel and mainly affected zero-voltage binding affinity for Ca^{2+}, by a factor of 1.4. A similar effect was demonstrated with the Ba^{2+} block of K^+ current in *Myxicola* giant axon (Schauf, 1983). Due to competition of H^+ (D^+) with Ca^{2+} for the binding sites, Ca^{2+} binding should be dependent on pH (pD). At pH = pD, deuterons bind more strongly compared to protons, which should result in the pK values for the acceptor groups shifting to a more alkaline region, whose extent is usually about 0.4–0.5 units for organic acids and bases (Lobyshev & Kalinichenko, 1978). To illustrate the effect of this D_2O-induced pK shift on Ca^{2+} binding affinity, we used two chelating agents with different pK values, below and above the experimental pH (pD) = 7.2, citric acid and EGTA, respectively (Fig. 1). In D_2O, the calculated values of apparent binding constants for Ca^{2+} at pH (pD) = 7.2 were decreased 10-fold for EGTA, which has two pK values in the alkaline region, and only 1.35-fold in the case of citric acid with the highest pK value of around 6. Since the magnitude of the latter effect was comparable to the isotope effect on the K^+ channel block by Ca^{2+}, the pK value of the acceptor group within a channel was expected to be slightly larger than 6.

Effect of D_2O on the Voltage- and Ca^{2+}-Dependent Channel Gating

The effect of H_2O/D_2O substitution on the channel open probability was found here to be a complex function of voltage and internal Ca^{2+}. Therefore, it was necessary for the description of the D_2O effect to model the channel voltage- and Ca^{2+}-dependent behavior in some detail. The model described below is based on two experimental facts. First, as demonstrated in Fig. 10, the apparent Ca^{2+} binding affinity was higher upon hyperpolarization and, thus, the voltage dependence of Ca^{2+} binding could not be explained by the Woodhull (1973) model. At −50 mV, k_d varied within different samples from 2–8 μM, and between −100 and 25 mV it changed from 0.5 to 12 μM (*cf.* Figs. 6 and 10). The absence of Ca^{2+} binding facilitation upon depolarization indicates weak or no voltage dependence. Moreover, a weak voltage dependence of Ca^{2+} binding to the K^+ channel was also found by Laver and Walker (1991) in *C. australis*. Second, as shown here, the channel half-activation voltage was shifted to more negative values by a decrease in Ca^{2+} concentration. This Ca^{2+}-dependent shift of the closed-open equilibrium can be explained in terms of preferential Ca^{2+} binding to the open channel conformation. These conditions could be expressed by the following reaction steps (on the left, with equilibrium constants for each step on the right):

(1) $C \leftrightarrow O$ $k_{co} = \exp(z\delta' F(V'_{1/2} - V)/RT)$
(2) $C^*n\mathrm{Ca} \leftrightarrow O^*n\mathrm{Ca}$ $k_{c^*o^*} = \exp(z\delta'' F(V''_{1/2} - V)/RT)$
(3) $C + n\mathrm{Ca} \leftrightarrow C^*n\mathrm{Ca}$ $k_{cc^*} = ([\mathrm{Ca}^{2+}]/k_{d(\mathrm{close})})^{\alpha}$
(4) $O + n\mathrm{Ca} \leftrightarrow O^*n\mathrm{Ca}$ $k_{oo^*} = ([\mathrm{Ca}^{2+}]/k_{d(\mathrm{open})})^{\alpha}$

where steps (1) and (2) describe the channel voltage-dependent close-open transitions in the absence and presence of bound Ca^{2+}, respectively, while steps (3) and (4) described Ca^{2+} binding to the closed and open conformations of the channel protein, respectively. Here, $V'_{1/2}$ or $V''_{1/2}$ are the midpoint potentials for the channel activation and $z\delta'$ or $z\delta''$ are the valences of the gating charge at zero or infinite Ca^{2+}, respectively, $k_{d(\mathrm{open})}$ or $k_{d(\mathrm{close})}$ are the constants for Ca^{2+} binding to the open or closed conformations, respectively, and α is the Hill coefficient. According to the principle of microscopic reversibility, $(k_{d(\mathrm{close})}/k_{d(\mathrm{open})})^{\alpha} = \exp(z\delta\ (V''_{1/2} - V'_{1/2})/RT) = \kappa$, when $V''_{1/2} > V'_{1/2}$ the binding of Ca^{2+} to the open conformation will be favorable.

The channel activation by hyperpolarization and by cytoplasmic Ca^{2+} could only be explained by weak voltage dependence of Ca^{2+} binding which, however, strongly influences the channel voltage dependence. All this is emphasized by the proposed model. The alternative model of Moczydlowski and Latorre (1983) which assumes that voltage dependence of channel kinetics directly reflects Ca^{2+} binding could certainly not explain the observed channel activation at steps to more negative potentials which are actually unfavorable for Ca^{2+} binding. Furthermore, the model underlines the shift of midpoint potential for channel activation as the main effect of Ca^{2+} concentration change and predicts two limiting states for the voltage dependence, at low and high Ca^{2+}, respectively (*see* Fig. 9 and its model parameters shown in Table 2).

The data points in the plot of $V_{1/2}$ values obtained in D_2O and H_2O against pCa (Fig. 9) were fitted using the above scheme, and the values of $V'_{1/2}$, $V''_{1/2}$, k_d and α were obtained. To test the validity of the above model, the parameters of Ca^{2+} binding in H_2O were also extracted from the independent experiment of Fig. 6. The values of $k_{d(\mathrm{open})}$ and α from these two types of experiments were found to be in good agreement (*see* legend to Fig. 6 and Table 2). The result of this analysis suggested that D_2O produced stronger cooperative interactions between Ca^{2+} binding sites, since the α value increased from approximately 1 in H_2O to 3 in D_2O (Table 2). However, these values were obtained by averaging the recordings from multichannel patches (5–15 channels in the patch). This could smear the pCa dependence of channel activity, providing activation by Ca^{2+} can vary between channels in one population. With the presently used preparation, even after attempts to reduce the patch area by making microelectrodes of high resistance (up to 50 MΩ), obtaining single channel recordings was not possible. Thus, although the D_2O effect is evident, the obtained α values could be underestimated.

The binding of Ca^{2+} to the open conformation weakened 10-fold in D_2O compared to H_2O, the binding constant values being 6 and 0.6 μM, respectively. In contrast, Ca^{2+} binding to the close conformation changed much less in D_2O, the binding constant values being twice smaller than in H_2O, 14 and 30 μM, respectively. A possible explanation for this finding would be that in the open channel conformation, pK values for Ca^{2+} accepting groups are in a more alkaline range compared to the closed conformation. Hence, according to the data on chelating agents, citric acid and EGTA (Fig. 1; *see above*) the isotope effect on Ca^{2+} binding would be larger in the open conformation. At a very low Ca^{2+} concentration, D_2O did not affect the channel voltage dependence in any way. In contrast, at the highest Ca^{2+} concentrations the shift of $V_{1/2}$ was as large as 60 mV. According to these data, the channel was sensitive to D_2O only with Ca^{2+} bound. Different Ca^{2+} binding to channel protein in D_2O compared to H_2O could affect channel conformation, particularly the conformation of its voltage gate, which would result in a different value of $V''_{1/2}$, measured in H_2O and D_2O.

The complex gating mechanism in the *Chara* K^+ channel, which was activated by voltage and by an agonist (Ca^{2+}), could account for the considerably larger effects of D_2O on the channel activity found here, compared to that for the channels regulated by voltage. (Conti & Palmieri, 1968; Schauf & Bullock, 1979; Schauf, 1983) or by binding of a ligand (Lewis, 1984). In its results, the present study resembles the case of D_2O effects on enzymatic processes with or without allosteric regulation (Henderson et al., 1970; Lobyshev & Kalinichenko, 1978). Namely, D_2O was shown to greatly affect the cooperative properties, rather than the primary catalytic step in allosteric enzymes. The rate of the overall enzymatic reaction could thus be changed by an order of magnitude in D_2O, compared to the change by a factor of less than 2, typical for the isotope effect on the primary reaction step.

Conclusions

The effect of H_2O/D_2O substitution on the single K^+ channel conductance in *C. gymnophylla* could be explained in terms of a solvent isotope effect, in agreement with previous results which showed that

the ion flow through the channel is limited by diffusion at the channel entrance (Laver et al., 1989; Pottosin, 1990). D_2O effects on cytosolic Ca^{2+} binding in the course of channel activation and blockage could be explained by the changes of pK values for the acceptor groups within the channel. The apparent number (α) of Ca^{2+} ions bound to the channel at the activation step was found to be as large as 3 in D_2O, which was close to the values obtained in H_2O for Ca^{2+}-activated K^+ channels of other origin. In *Chara* the value of α in H_2O was found to be approximately 1. It appeared that H_2O/D_2O substitution mainly affected the modulation of channel voltage dependence by Ca^{2+}, rather than the voltage dependence itself. This could account for the substantially larger effect of D_2O on the kinetics of the K^+ channel in *Chara*, compared to its effects on other voltage-dependent ionic channels.

We wish to express our gratitude to Dr. A.A. Alexandrov and Dr. A.A. Kataev for valuable discussions.

References

Andersen, O.S. 1983. Ion movement through gramicidin A channels. Studies on the diffusion-controlled association step. *Biophys. J.* **41**:147–165

Andjus, P.R., Vučelić, D. 1990. D_2O-induced cell excitation. *J. Membrane Biol.* **115**:123–127

Andjus, P.R., Vučelić, D., Kataev, A.A., Pottosin, I.I., Alexandrov, A.A., Berestovsky G.N. 1990. D_2O/H_2O exchange at the *Characean* cell membrane: transport mechanisms and the solvent isotope effect. *Studia biophysica* **138**:105–114

Bertl, A. 1989. Current-voltage relationships of a sodium-sensitive potassium current in the tonoplast of *Chara corallina*. *J. Membrane Biol.* **109**:9–19

Brink, P.R. 1983. Effect of deuterium oxide on junctional membrane channel permeability. *J. Membrane Biol.* **71**:79–87

Budak, B.M., Samarsky, A.A., Tichonov, A.N. 1956. A Book of Problems in Mathematical Physics. State Publishers of Technical and Theoretical Literature, Moscow (*in Russian*)

Conti, F., Palmieri, L. 1968. Nerve fiber behaviour in heavy water under voltage-clamp. *Biophysik* **5**:71–77

Dainty, J., Hope, A.B. 1959. The water permeability of cells of *Chara australis*. *Australian J. Biol. Sci.* **12**:136–145

Durham, A.C.H. 1983. A survey of readily available chelators for buffering calcium ion concentrations in physiological solutions. *Cell Calcium* **4**:33–46

Finkelstein, A. 1987. Water Movement through Lipid Bilayers, Pores, and Plasma Membranes. Theory and Reality. Wiley-Interscience Publication, New York, Chichester, Brisbane, Toronto, Singapore

Hamill, O.P., Marty, A., Neher, E., Sakmann, B., Sigworth, F.J. 1981. Improved patch-clamp techniques for high-resolution recordings from the cells and cell-free membrane patches. *Pfluegers Arch.* **391**:85–100

Henderson, R.F., Henderson, T.R., Woodfin, B.M. 1970. Effects of D_2O on the association-dissociation rate in subunit proteins. *J. Biol. Chem.* **245**:3733–3737

Laver, D.R. 1990. Coupling of K^+-gating and permeation with Ca^{2+} block in the Ca^{2+}-activated K^+ channel in *Chara australis*. *J. Membrane Biol.* **118**:55–67

Laver, D.R., Fairley, K.A., Walker, N.A. 1989. Ion permeation in a K^+ channel in *Chara australis:* Direct evidence for diffusion limitation of ion flow in a maxi-K channel. *J. Membrane Biol.* **108**:153–164

Laver, D.R., Walker, N.A. 1987. Steady-state voltage-dependent gating and conduction kinetics of single K^+ channels in the membrane of cytoplasmic drops of *Chara australis*. *J. Membrane Biol.* **100**:31–42

Laver, D.R., Walker, N.A. 1991. Activation by Ca^{2+} and block by divalent ions of the K^+ channel in the membrane of cytoplasmic drops from *Chara australis*. *J. Membrane Biol.* **120**:131–139

Lewis, C.A. 1984. Deuterium oxide effects on frog endplate channels. *Biophys. J.* **45**:16–18

Lindley, B.D., Hoshiko, T., Leb, D.E. 1964. Effects of D_2O and osmotic gradients on potential and resistance of the isolated frog skin. *J. Gen. Physiol.* **47**:773–793

Lobyshev, V.I., Kalinichenko, L.P. 1978. Isotopic effects of D_2O in biology. S.E. Shnol, editor. Nauka Publishers, Moscow (*in Russian*).

Lühring, H. 1986. Recording of single K^+ channels in the membrane of cytoplasmic drop of *Chara australis*. *Protoplasma* **133**:19–28

Moczydlowski, E., Latorre, R. 1983. Gating kinetics of Ca^{2+}-activated K^+ channels from rat muscle incorporated into planar lipid bilayers. *J. Gen. Physiol.* **82**:511–542

Pottosin, I.I. 1990. Voltage- and Ca^{2+}-regulated K^+ channel in the tonoplast of *Characean* algae. *Studia biophysica* **138**:119–126

Schauf, C.L. 1983. Solvent substitution as a probe of gating processes in voltage-dependent ion channels. *In*: Structure and Function in Excitable Cells. D.C. Chang, I. Tasaki, W.J. Adelman, Jr., and H.R. Leuchtag, editors. pp. 347–363. Plenum, New York

Schauf, C.L., Bullock, J.O. 1979. Modifications of sodium channel gating in *Myxicola* giant axon by deuterium oxide, temperature and internal cations. *Biophys. J.* **27**:193–208

Tichonov, A.N., Samarsky, A.A. 1966. Equations of Mathematical Physics. Nauka Publishers, Moscow (*in Russian*)

Wayne, R., Tazawa, M. 1990. Nature of the water channels in the internodal cells of *Nitellopsis*. *J.Membrane Biol.* **116**:31–39

Woodhull, A.M. 1973. Ionic blockade of sodium channels in nerve. *J. Gen. Physiol.* **61**:687–708

Appendix

Diffusion of Water Through the Patch Membrane

Immediate H_2O/D_2O replacement in the bath initiates the influx of D_2O into the patch pipette and efflux of H_2O into the bath. The sum of volume fractions of water and heavy water is constant by definition, $C_v^H + C_v^D = 1$. Assuming that the fluxes of H_2O and D_2O are in opposite directions, noninteracting, and having equal magnitudes[1], the fractional composition of solvent at two sides of the patch was calculated as a function of time. To solve this function, two problems were considered: (i) diffusion of water in the volume external to the patch (for simplicity we assumed that the volume flux J originated from a spherical membrane with the area S_m equal to the area of the patch); and (ii) axial diffusion of water within a micropipette tip which was assumed to be of cylindrical form.

Water Efflux

Considering the case of radial diffusion with its rate (v) defined as

$$v = Cr$$

where C is concentration (volume fraction of H_2O) and r is radial distance, the diffusional equation becomes

$$\frac{\delta v}{\delta t} = D\frac{\delta^2 v}{\delta r^2} \tag{1A}$$

where D is the diffusion constant. If the flux J at $r = r_o$ ($S_m = 4\Pi r_o^2$) is constant, then

$$v(r_o, t) = \frac{J}{4\Pi D} = v_o \tag{2A}$$

and at the initial moment

$$v(r, 0) = 0, r \geq r_o \tag{3A}$$

the solution of this problem is (Tichonov & Samarsky, 1966):

$$v(r, t) = \frac{J}{4\Pi D}\left[1 - \frac{2}{\sqrt{\Pi}}\mathrm{erf}\left(\frac{r}{2\sqrt{(Dt)}}\right)\right]. \tag{4A}$$

For short times

$$J \approx C_o P S_m = P S_m \tag{5A}$$

where $C_o = 1$ is the initial volume fraction of H_2O at the inner side of the patch, P is the permeability coefficient for water diffusion through the patch. Therefore, for the volume fraction of H_2O at the external surface of patch membrane, $r = r_o$ we have

$$C(r_o, t) = \frac{Pr_o}{4D}\left[1 - \frac{2}{\sqrt{\Pi}}\mathrm{erf}\left(\frac{r_o}{2\sqrt{(Dt)}}\right)\right]. \tag{6A}$$

On putting $P = 1.5 \cdot 10^{-2}$ cm sec^{-1} (which is the upper limit for *Chara* membranes; Dainty & Hope, 1959; *see below*), $D = 2 \cdot 10^{-5}$ cm^2 sec^{-1} and $r_o = 10^{-4}$ cm, follows:

$$C(r_o, t) \leq \frac{Pr_o}{4D} = 0.02. \tag{7A}$$

Since H_2O efflux from the electrode decreased with time due to the decrease of H_2O fraction at the inner side, the estimate given by Eq. (7A) is the upper limit. Therefore, dilution of D_2O with H_2O at the external side of the patch will be negligible at any moment.

Diffusion in Patch Electrode

The patch electrode is considered as a semi-infinite cylinder with impermeable walls, initially filled with the H_2O solution, in which diffusion is everywhere axial. Equation (1A) has to be solved for the boundary condition, which, in the absence of significant accumulation of H_2O at the external side of the patch as shown above, can be written as

$$\left.\frac{\delta C}{\delta x}\right|_{x=0} = hC(0, t), t > 0 \tag{8A}$$

where $h = P/D$, and the initial condition is

$$C(x, 0) = \mathrm{const} = 1, x \geq 0. \tag{9A}$$

The solution of this problem is given (Budak, Samarski & Tichonov, 1956) as:

$$C(x, t) = \frac{2}{\sqrt{\Pi}}\mathrm{erf}\left(\frac{x}{2\sqrt{(Dt)}}\right) + \exp(hx + h^2 Dt)\left[1 - \frac{2}{\sqrt{\Pi}}\mathrm{erf}\left(\frac{x}{2\sqrt{(Dt)}} + h\sqrt{(Dt)}\right)\right]. \tag{10A}$$

For the volume fraction of H_2O at the internal membrane surface ($x = 0$) Eq. (10A) reduces to

$$C(0, t) = \exp(h^2 Dt)\left[1 - \frac{2}{\sqrt{\Pi}}\mathrm{erf}(h\sqrt{(Dt)})\right]. \tag{11A}$$

In Fig. 11 curves of volume fractions of H_2O and D_2O on the internal membrane surface are plotted against time for different values of permeability coefficient. The diffusion coefficient for water (P_d) could not be correctly determined in the large cells of *Charophytes*, thus we used the value of osmotic water permeability $P_f = 1.5 \cdot 10^{-2}$ cm sec^{-1} obtained with these cells as the upper limit for P_d (Dainty & Hope, 1959; Wayne & Tazawa, 1990) since the ratio P_f/P_d is always greater than 1 for a porous membrane. The largest P_f/P_d ratio measured in a living cell is about 6 for red blood cells (Finkelstein, 1987), and thus, a sixfold smaller value than P_f was used as the lower limit for P_d in *Chara*, namely, $2.5 \cdot 10^{-3}$ cm sec^{-1}.

[1] The last two assumptions are approximations to an ideal case, used only for estimative calculations.